

Journal: Nature Medicine

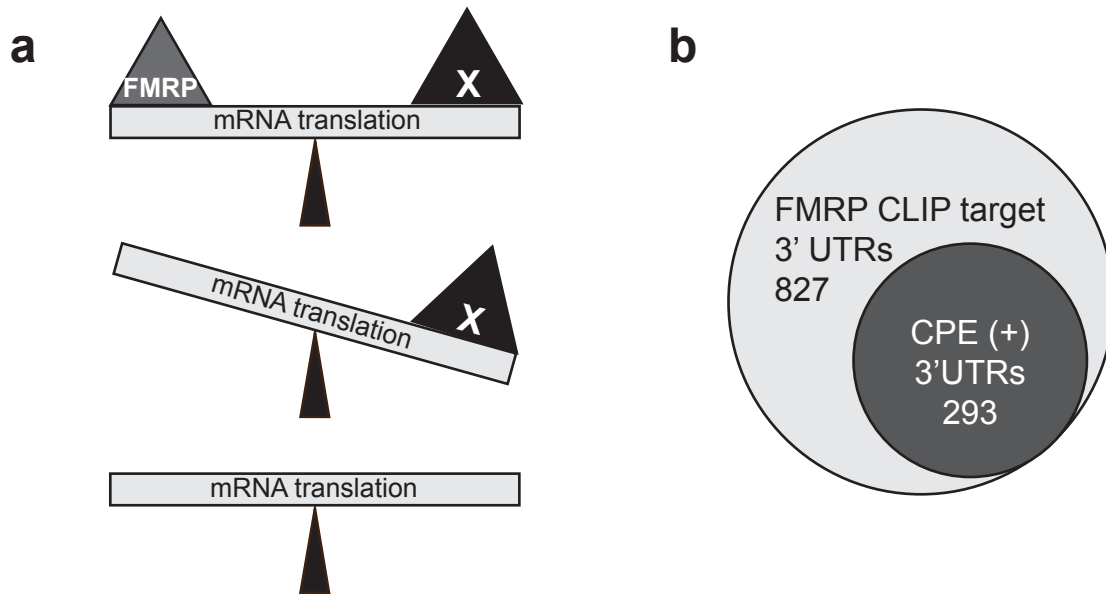
Article Title:	Genetic and Acute CPEB Depletion Ameliorate Fragile X Pathophysiology
Corresponding Author:	Joel D. Richter

Supplementary Item & Number	Title or Caption
Supplementary Figure 1	Balance of translation in the brain
Supplementary Figure 2	Co-localization and co-purification of CPEB and FMRP
Supplementary Figure 3	Generation of <i>Fmr1</i> ^{-y} <i>Cpeb</i> ^{-/-} double knockout (DKO) mice
Supplementary Figure 4	Impaired glycine-induced long-term potentiation (Gly-LTP) in <i>Fmr1</i> KO animals is rescued in DKO
Supplementary Figure 5	Rescued spine density and body weight in DKO animals
Supplementary Figure 6	<i>In vitro</i> synaptic formation in cultured hippocampal and cortical neurons
Supplementary Figure 7	<i>Cpeb</i> deletion ameliorates FXS-associated behavioral abnormalities
Supplementary Figure 8	FMRP affects translation elongation
Supplementary Table 1	Putative CPEs within FMRP target mRNA 3' UTRs (see Excel file)
Supplementary Table 2	Western Blot analysis of <i>Fmr1</i> KO, <i>Cpeb</i> KO and DKO hippocampi, relative to WT
Supplementary Table 3	Western Blot analysis of <i>Fmr1</i> KO cortex, relative to WT
Supplementary Table 4	Additional details of statistical analysis for RTR assay
Supplementary Table 5	Summary of FXS-related Phenotypes in DKO animals
Supplementary Table 6	Antibodies used for Western Blot analysis in this study
Supplementary Methods	

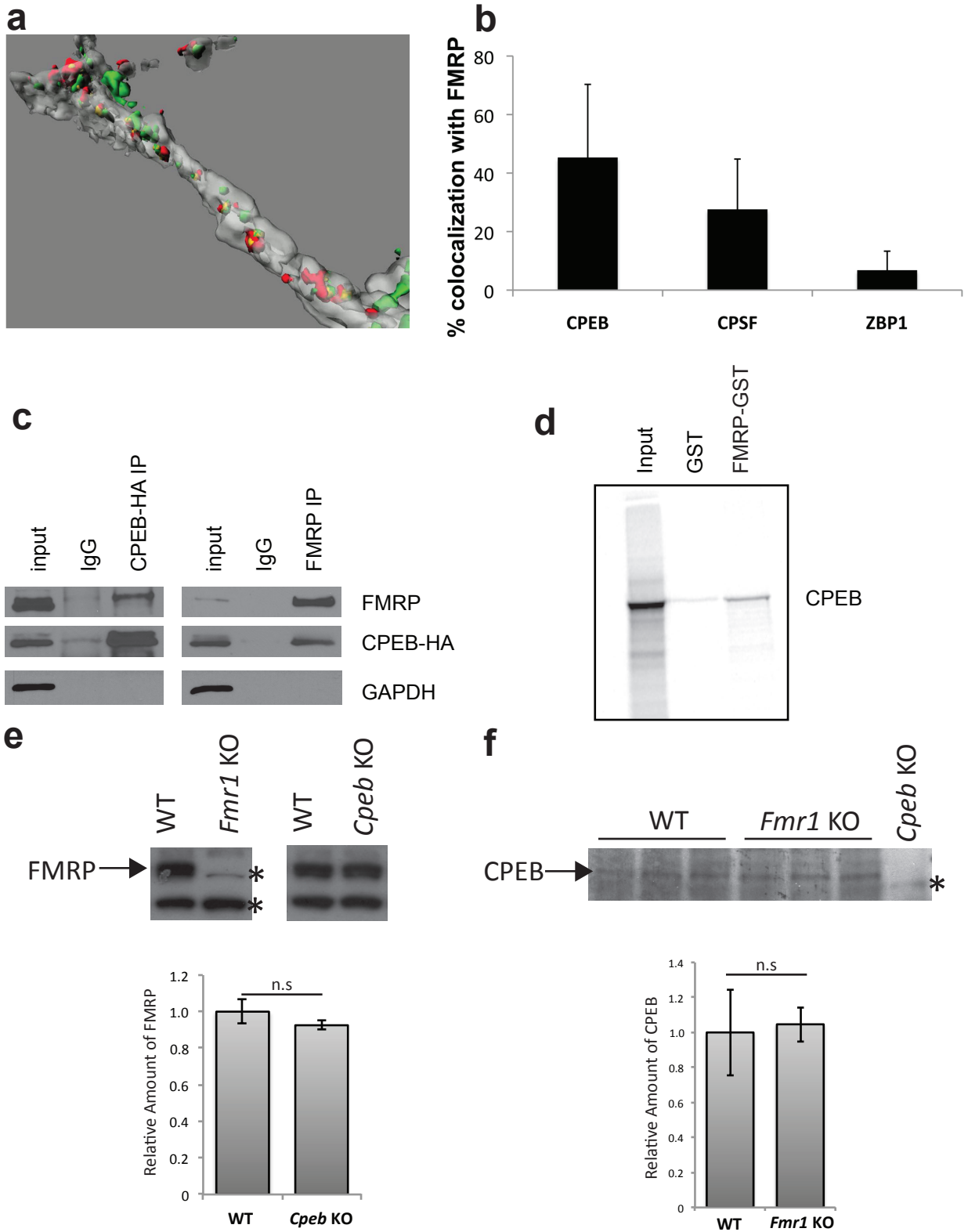
Supplementary Information for:

Genetic and Acute CPEB Depletion Ameliorate Fragile X Pathophysiology

Tsuyoshi Udagawa^{1,8,*}, Natalie G. Farny^{1,*}, Mira Jakovcevski^{2,9,*}, Hanoch Kaphzan^{3,10}, Juan Marcos Alarcon⁴, Shobha Anilkumar⁵, Maria Ivshina¹, Jessica A. Hurt⁶, Kentaro Nagaoka^{1,11}, Vijayalaxmi C. Nalavadi⁷, Lori J. Lorenz¹, Gary J. Bassell⁷, Schahram Akbarian^{2,12}, Sumantra Chattarji⁵, Eric Klann³, and Joel D. Richter^{1,%}



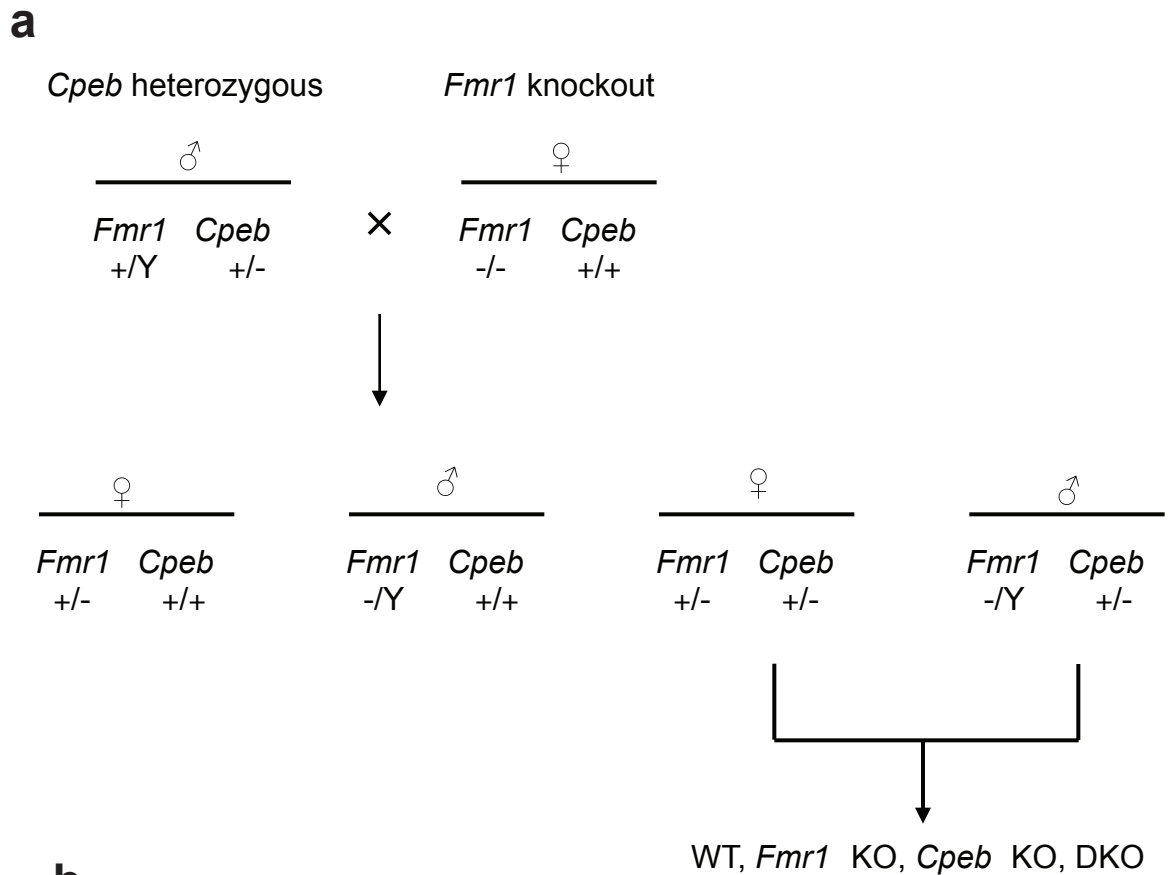
Supplementary Figure 1: Balance of translation in the brain. **a**, A translational homeostasis model where FMRP and a factor “X” balance translation in the brain. When FMRP is absent, the protein synthesis increase is manifested by FXS. When both FMRP and factor “X” are absent, translation is re-balanced and normal neural activity is restored. **b**, Of the 827 FMRP CLIP targets, 293 have putative candidate CPEs in their 3’ UTRs.



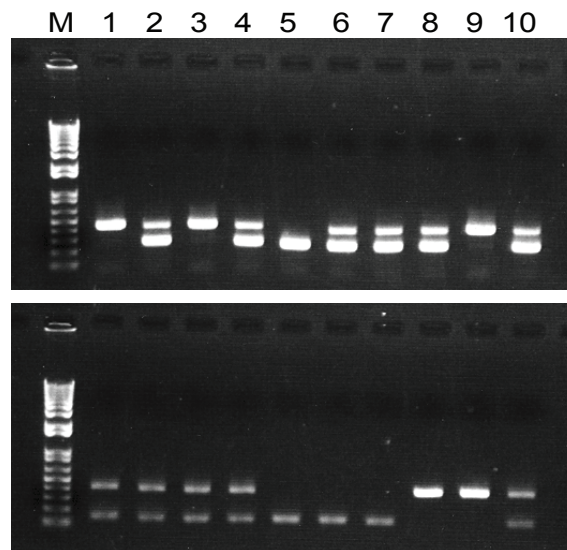
Supplementary Figure 2: Co-localization and co-purification of CPEB and FMRP.

a, Co-localization of FMRP and CPEB in dendrites. Isosurface (Bitplane) reconstruction of multiple slices of a typical dendritic segment 50 μ m away from the cell body stained with CPEB(red) and FMRP(green). Co-localized pixels are shown in yellow. Morphology of the neuron was revealed by staining of F-actin with Alexa488-labelled phalloidin (gray).

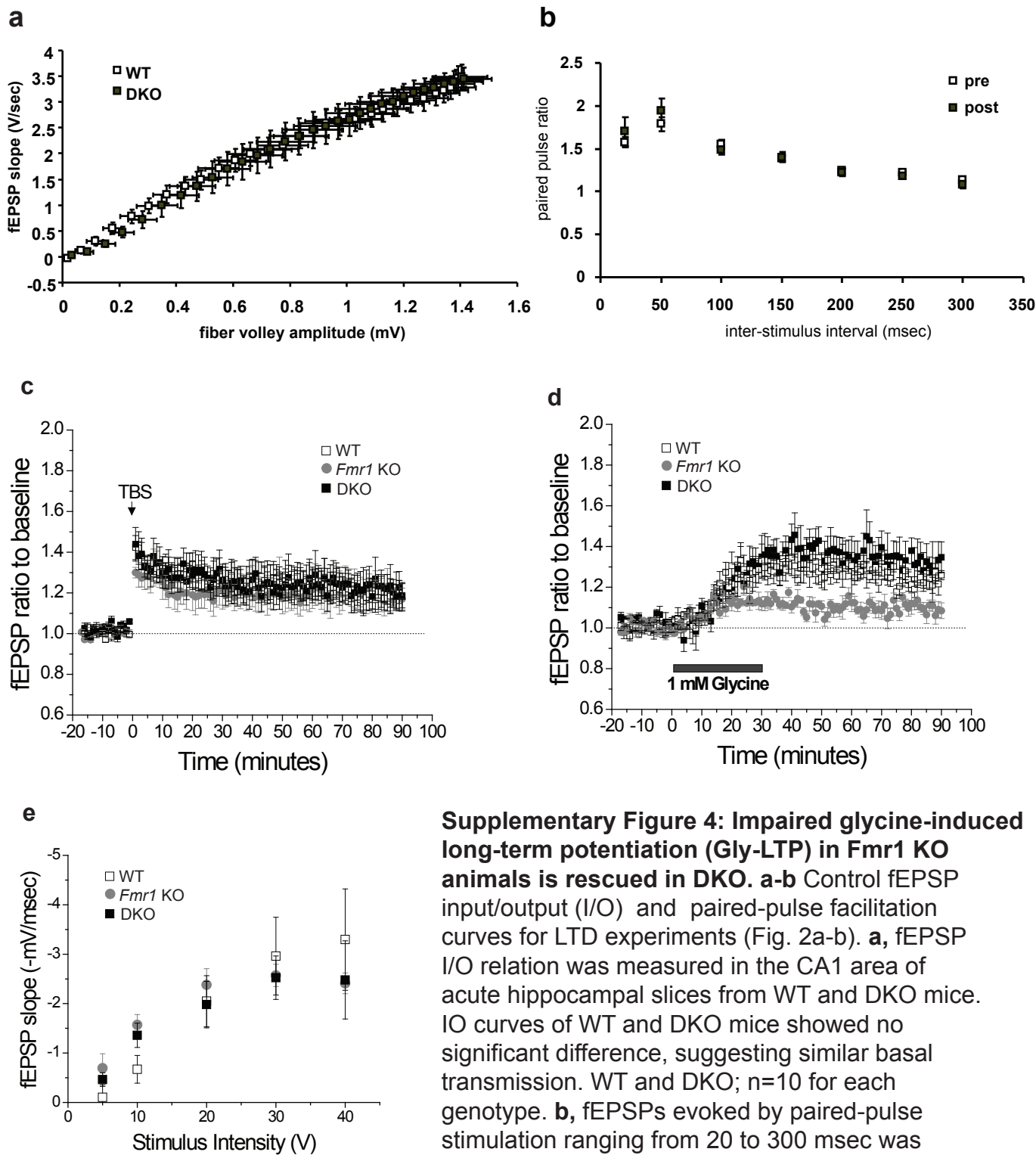
b, Quantification of co-localization of FMRP with CPEB, CPSF or an unrelated RNA binding protein ZBP1 from multiple neurons. Error bars are +/- S.D. **c**, HA-CPEB-encoding DNA was transfected into Neuro2A cells, followed by HA immunoprecipitation and western blotting for FMRP, CPEB, and as a negative control, GAPDH. Immunoprecipitation with non-specific IgG served as a negative control. A reciprocal co-immunoprecipitation experiment with FMRP was also performed. **d**, In vitro synthesized ³⁵S-methionine-labeled CPEB was subjected to chromatography on GST-agarose or GST-FMRP-agarose, followed by elution and SDS-PAGE to detect CPEB. **e-f**, Levels of FMRP are unaffected in Cpeb KO animals, and levels of CPEB are unaffected in Fmr1 KO animals. **e**, FMRP was compared by Western blot in WT and Cpeb KO hippocampal lysates. Representative blots are shown. No difference was detected in FMRP levels between the genotypes (n.s. = not significant, Student's t test, n=6-7). **f**, CPEB was compared by Western blot in WT and Fmr1 KO testes lysates. Testes contain high levels of CPEB, and we have found that CPEB is poorly detected by Western blot in other tissues. No difference was detected in CPEB levels between genotypes (n.s.= not significant, Student's t test, n=3). Error bars are S.E.M. * indicates non-specific bands.



b

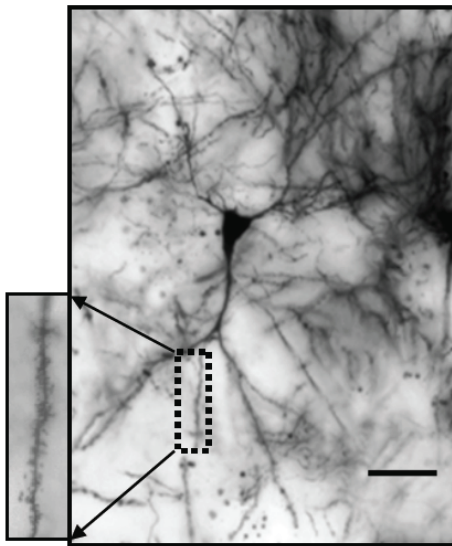
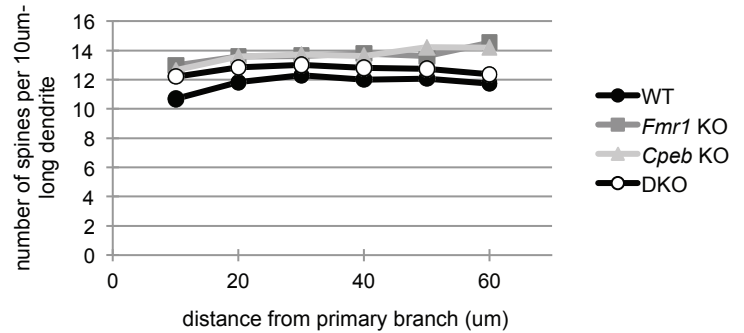
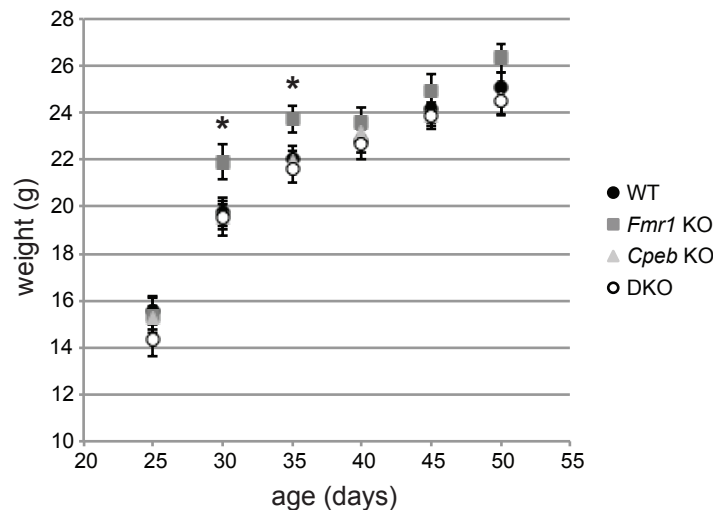


Supplementary Figure 3: Generation of *Fmr1* $-/y$ *Cpeb* $-/-$ double knockout (DKO) mice.
a, Breeding strategy. *Cpeb* heterozygous males (*Cpeb* $+/-$) were crossed with *Fmr1* knockout (KO) females (*Fmr1* $-/-$). The offspring include *Fmr1* $+/-$ *Cpeb* $+/-$ females and *Fmr1* $-/y$ *Cpeb* $+/-$ males. This pair was used to generate WT, *Fmr1* KO, *Cpeb* KO and DKO males for these experiments. **b**, Representative PCR genotyping of *Fmr1* KO and *Cpeb* KO mice. Upper and lower gels show *Fmr1* and *Cpeb* genotypes, respectively. In both case, upper and lower bands indicate mutated and wild type locus, respectively. Animal #9 represents the DKO.

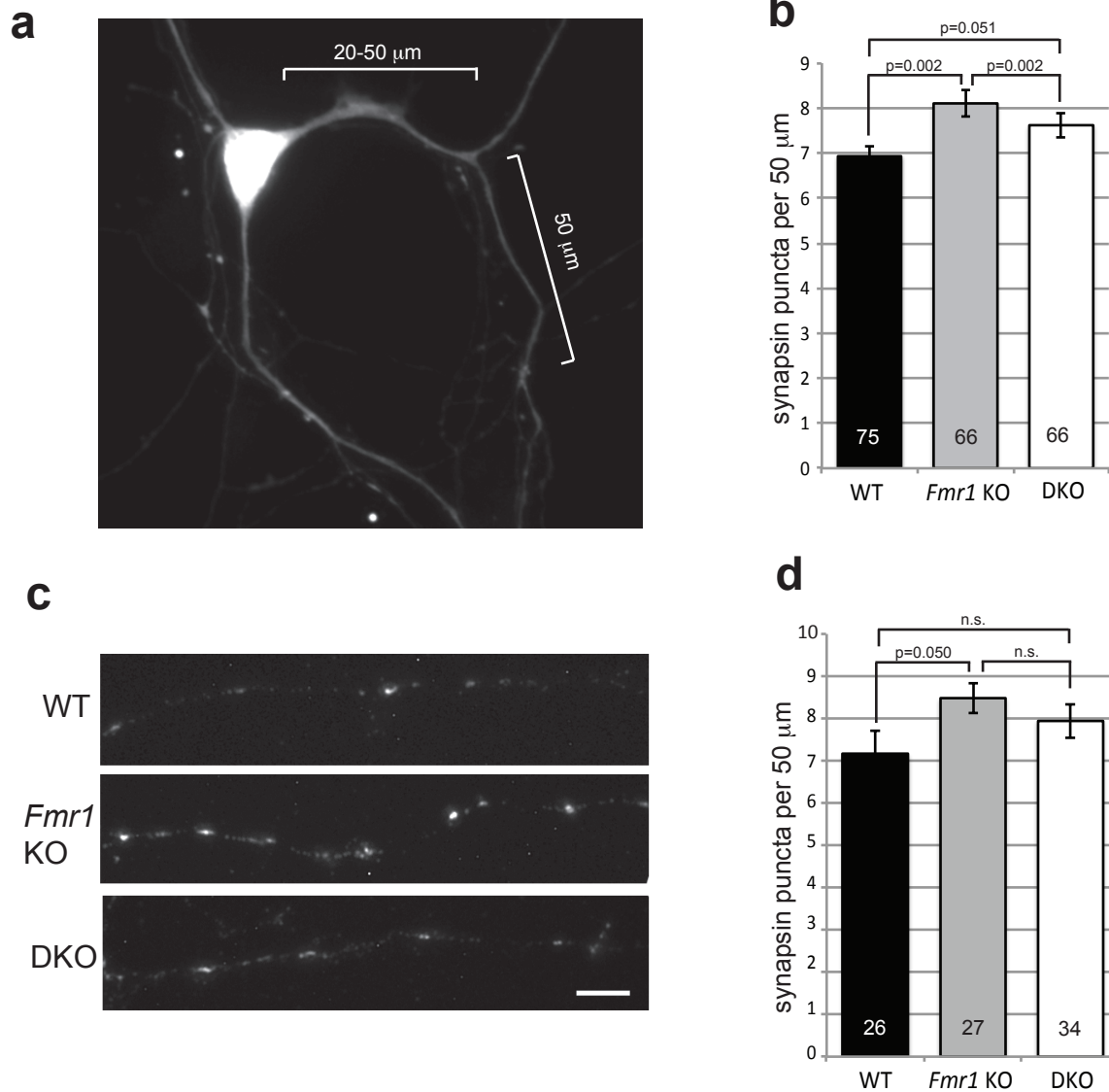


Supplementary Figure 4: Impaired glycine-induced long-term potentiation (Gly-LTP) in *Fmr1* KO animals is rescued in DKO. **a-b** Control fEPSP input/output (I/O) and paired-pulse facilitation curves for LTD experiments (Fig. 2a-b). **a**, fEPSP I/O relation was measured in the CA1 area of acute hippocampal slices from WT and DKO mice. IO curves of WT and DKO mice showed no significant difference, suggesting similar basal transmission. WT and DKO; n=10 for each genotype. **b**, fEPSPs evoked by paired-pulse stimulation ranging from 20 to 300 msec was recorded in the CA1 area of acute hippocampal slices. The paired pulse facilitation curve of DKO

mice before (baseline) and 60 minutes after DHPG application showed no significant difference, suggesting a post-synaptic mechanism for electrophysiological rescue. WT and DKO, n=10. **c-e**, Long term potentiation (LTP) at Schaffer collateral-CA1 synapses, n=5 for each genotype. **c**, LTP induced by theta burst stimulation (TBS-LTP) was unaffected in *Fmr1* KO and DKO animals. **d**, LTP induced by application of 1mM glycine (Gly-LTP) was impaired in *Fmr1* KO animals, but restored to WT level in DKO animals. **e**, fEPSP I/O relation in hippocampal slices used for LTP analysis was similar among WT, *Fmr1* KO and DKO animals. Error bars are +/- S.E.M.

a**b****c**

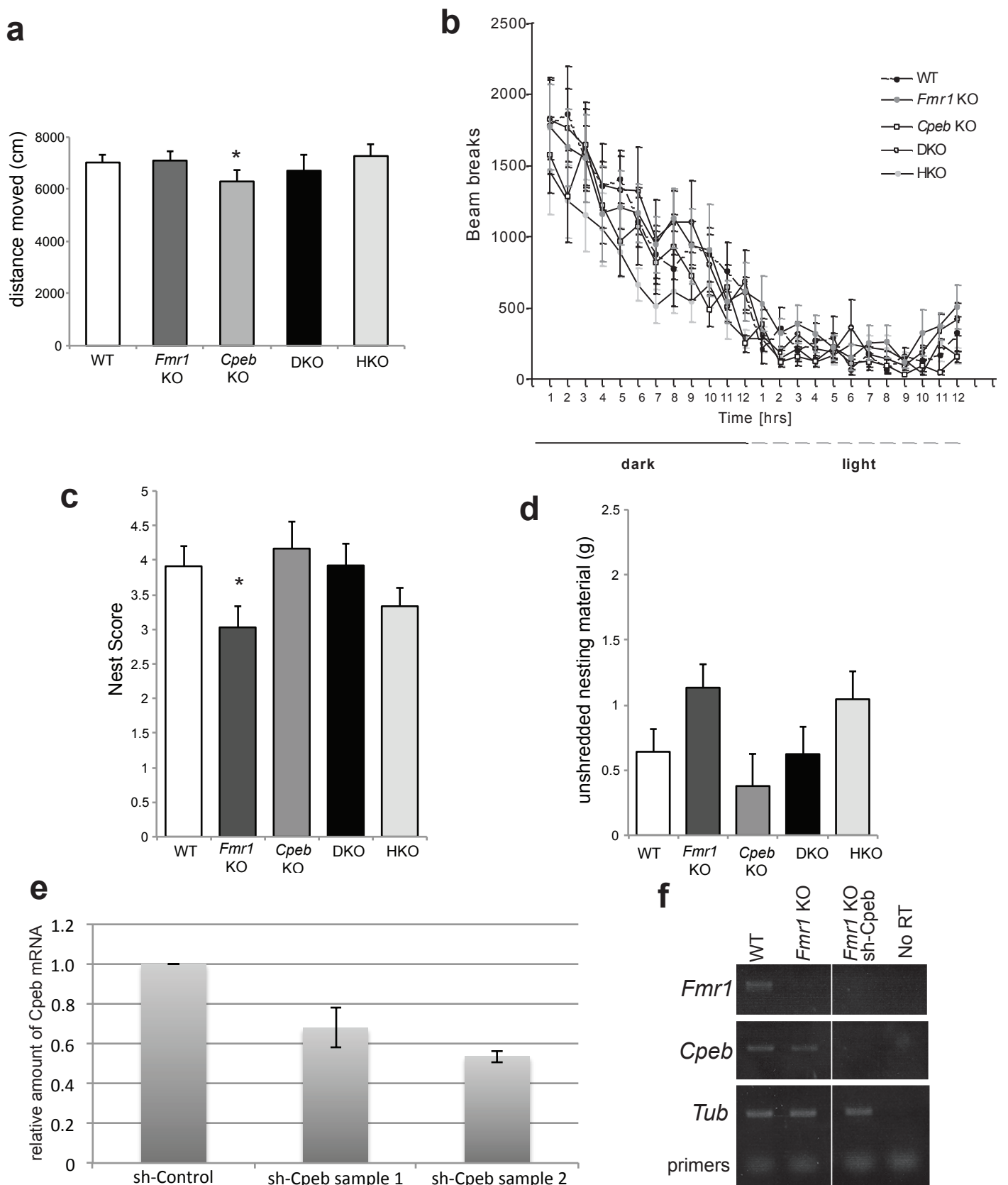
Supplementary Figure 5: Rescued spine density and body weight in DKO animals **a**, Low-power photomicrograph of a Golgi-Cox stained neuron (20x magnification) in the CA1 area of hippocampus (scale bar, 20 μm.) The inset shows an image of spines on a dendritic segment from the same neuron. **b**, Segmental analysis of spine density along a primary dendritic branch of pyramidal neurons in the CA1 area of hippocampus. Total number of spines along dendritic branch was expressed for 10 μm segments starting from the origin of the branch up to 60 μm from the origin. **c**, Body weight of each genotype was measured at the indicated postnatal ages and compared to WT. At P30 and P35, body weight of Fmr1 KO (n=15) was increased compared to WT (n=16; *p<0.05, students t-test), while Cpeb KO (n=17) and DKO (n=19) were indistinguishable from WT (p>0.05, students t-test).



Supplementary Figure 6: *In vitro* synaptic formation in cultured hippocampal and cortical neurons.

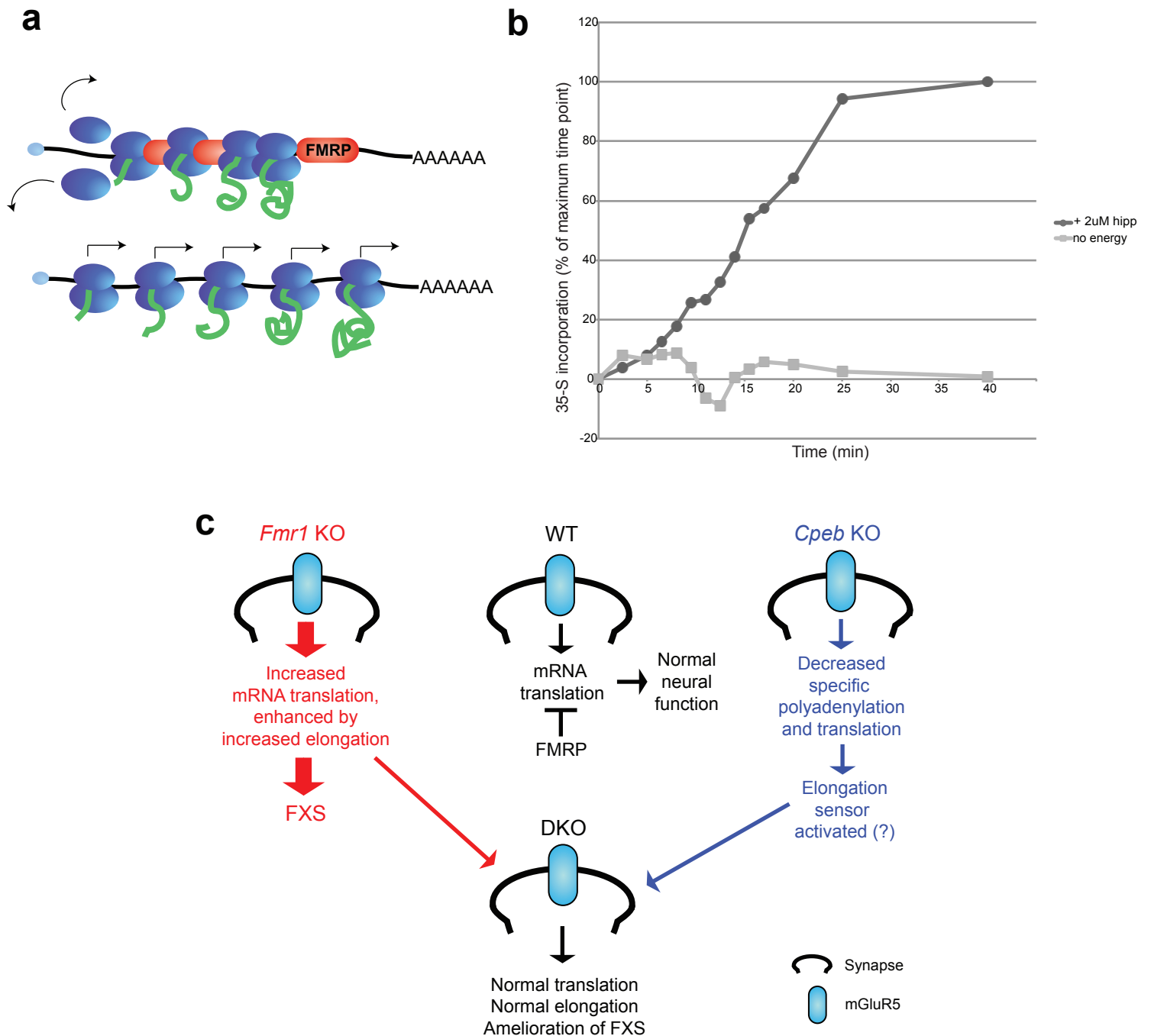
a, 40x image of a DIV 11 cortical neuron, transfected with GFP for visualization. For quantification of synapsin puncta, 50 μm segments of secondary dendrites that branched from a primary dendrite at 20-50 μm from the cell body were chosen for analysis. **b**, **d**, Synapsin puncta per 50 μm were counted in DIV7-8 hippocampal neurons (**b**) or DIV 11 cortical neurons (**d**) of the indicated genotypes. n values are listed in each bar. Student's t test was used to calculate the p values shown.

c, Representative images of secondary dendrites stained with synapsin antibody. Bar = 5 μm .



Supplementary Figure 7: *Cpeb* deletion ameliorates FXS-associated behavioral abnormalities. **a**, Locomotor activity measured as total distance moved in the open field arena during the test session (n=9-11, ANOVA, $F(4,46)=1.98$, n.s.). **b**, Locomotor activity was measured using a photobeam activity system for 24 h. There was no difference among the genotypes (n=9-11). **c-d**, nest building

ability was assessed in five genotypes after 72 hours. (c) Nests were scored on a scale of 1 to 5 and (d) unused nesting material was weighed 72 hours after presenting the animals with a 2.5g nestlet. $n=9-18$, ANOVA, $F(4,70)=2.32$, $p=0.065$ and $F(4,70)=2.21$, $p=0.076$, respectively. $*p<0.05$, as compared to wild-type mice (Mann Whitney U test). **e-f**, quantitative RT-PCR (e) and semi-quantitative RT-PCR (f) analysis of Cpeb mRNA levels in hippocampal samples from WT, Fmr1 KO and Fmr1 KO injected with sh-Control or sh-Cpeb virus, as indicated. Samples were microdissected from the combined CA1 and dentate gyrus regions of 500 μm thick coronal brain sections. Error bars are S.E.M. of four technical replicates of the RT-qPCR reaction for each sample.



Supplementary Table 2: Western Blot analysis of *Fmr1* KO, *Cpeb* KO and DKO hippocampi, relative to WT

Western blot signal, relative to WT

antibody:	<i>Fmr1</i> KO	<i>Cpeb</i> KO	DKO	FMRP CLIP target ⁺	CPE [§]
Arc/Arg3.1	1.192078199	0.930396623	1.013940941	N	-
eEF1A2	1.194528186	1.133330076	1.308099972	Y	N
Map1b	1.069366344	0.663031341	0.83575083	Y	Y
Map2	1.017390045	0.690356114	1.387541291	Y	N
NR2a	1.682986544	0.928270137	1.11586291	Y	Y*
PSD-95	1.043130828	1.00711371	1.064521236	Y	Y
PTEN	0.904021988	0.684914164	0.64472197	Y	Y
Pum2	1.348008244	0.819665149	0.830767284	Y	N
STEP	1.096513611	1.177117957	0.77906754	Y	Y
Synapsin	1.61238691	0.751530235	1.120930375	Y	N
p-GSK3a	1.113341198	0.97889839	1.071636575	-	-
Total GSK3a	1.014071386	0.972032253	0.807562333	N	-
p-P70S6K1 421/424	0.874378392	1.315055379	1.199517306	-	-
p-P70S6K1 389	1.164424196	1.429832313	1.497866447	-	-
Total S6K1	1.093284018	0.964731135	0.980485244	N	-
p-AKT 473	0.893946799	0.681452664	0.848753167	-	-
p-AKT 308	0.590390614	0.648837273	0.634546533	-	-
Total AKT	1.097161072	1.107429872	1.12414638	N	-
p-ERK1/2	1.145184278	1.053893986	0.990291881	-	-
Total Erk1/2	1.010660656	0.892051526	1.065309762	Y	Y
p-RPS6	1.261426555	0.785424808	0.963572741	-	-
Total rpS6	1.054116293	1.029430162	1.06076689	N	-
p-eEF2	0.972607612	1.144366885	0.993351832	-	-
total eEF2	1.087057923	0.959729096	0.860470182	Y	N

n=10-12 animals per genotype, males, 6 weeks of age

Green shading, increase versus WT, p<0.05; Light green shading, increase versus WT, p<0.09; Red shading, decrease versus WT, p<0.05; Light red shading, decrease versus WT, p<0.09 (student's T test, WT x genotype).

⁺ FMRP CLIP targets were defined as those mRNAs identified by Darnell et al⁷. Dash (-) indicates that the CLIP target designation is not relevant for this antibody (phospho-specific antibodies).

[§] CPEs were defined as UUUUAU or UUUUAAU sequences within 300nt of the end of the transcript. See Online Methods for further details of bioinformatics analysis. Dash (-) indicates that this mRNA was not analyzed for CPEs because it was not a CLIP target.

* The *Grin2a* (encoding NR2a) 3' UTR is incomplete in the RefSeq database used for these analyses. Other analysis has demonstrated that this gene does contain a valid CPE¹⁸.

Supplementary Table 3: Western Blot analysis of *Fmr1* KO cortex, relative to WT

antibody:	Western blot signal, <i>Fmr1</i> KO/WT
Arc/Arg3.1	1.234566398
eEF1A2	0.841809728
Map1b	1.094425511
NR2a	*0.684433729
PSD-95	0.991582322
Synapsin	0.681879348
p-RPS6	0.614234336
Total rpS6	0.939735436

n=3-4 animals per genotype, 2.5-6 months of age, *p<0.05.

Supplementary Table 4: Additional details of statistical analysis for RTR assay.

timepoint (minutes)	ANOVA p=	Post hoc* (WT vs. FKO) p<0.05	Post hoc* (Fmr1KO vs. DKO) p<0.05	Post hoc* (WT vs. DKO) p<0.05	F _(3,13)
8	0.012	Y	Y	N	6.104
9.5	0.02	N	Y	N	5.184
11	0.015	Y	Y	N	5.776
12.5	0.027	N	Y	N	4.724
14	0.064	N	Y	N	3.345

*Bonferroni post hoc analysis (<http://graphpad.com/quickcalcs/posttest1.cfm>)

Y, yes (p is <0.05); N, no (p is not <0.05)

Supplementary Table 5: Summary of FXS-related Phenotypes in DKO animals

Phenotype in <i>Fmr1</i> KO	Rescued in DKO?
Electrophysiological <ul style="list-style-type: none"> • enhanced LTD • impaired LTP 	<ul style="list-style-type: none"> • Yes, but no longer protein synthesis-dependent • Yes when induced by glycine, no defect in TBS-LTP but <i>Cpeb</i> KO defect is rescued
Morphological <ul style="list-style-type: none"> • hippocampal spine density • <i>In vitro</i> hippocampal and cortical synapse formation • body weight 	<ul style="list-style-type: none"> • Yes (partial) • Yes (partial) • Yes
Behavioral <ul style="list-style-type: none"> • audiogenic seizure • locomotor activity • anxiety in open field • passive avoidance • working memory • nest building 	<ul style="list-style-type: none"> • Yes (partial) • no defect in <i>Fmr1</i> KO • Yes • no defect in <i>Fmr1</i> KO, but <i>Cpeb</i> KO defect is rescued • Yes, both genetic and acute • Yes
Biochemical <ul style="list-style-type: none"> • bulk protein synthesis • specific protein synthesis • translation elongation rate 	<ul style="list-style-type: none"> • Yes • Yes, for some targets • Yes

Supplementary Table 6: Antibodies used for Western Blot analysis in this study

Antibody	Company/Catalog #	Dilution
Arc/Arg3.1	Santa Cruz Biotechnology/sc-17839	1:500
eEF1A2	Abcam/ab37969	1:1000
Map1b	Santa Cruz Biotechnology/sc-25729	1:200
Map2	Millipore/AB5622	1:10,000
NR2a	Millipore/05-901R	1:500
PSD-95	Abcam/ab2723	1:1000
PTEN	Cell Signaling Technology/9556	1:500
Pum2	Bethyl/A300-202A	1:500
STEP	kind gift of P. Lombroso, Yale Univ.	1:1000
Synapsin1	Abcam/ab64581	1:1000
p-GSK3a S21	Cell Signaling Technology/9316	1:1000
Total GSK3a	Cell Signaling Technology/4337	1:1000
p-P70S6K1 T421/S424	Cell Signaling Technology/9204	1:500
p-P70S6K1 T389	Cell Signaling Technology/9234	1:500
Total S6K1	Cell Signaling Technology/2708	1:1000
p-AKT S473	Cell Signaling Technology/9271	1:500
p-AKT T308	Cell Signaling Technology/9275	1:500
Total AKT	Cell Signaling Technology/9272	1:1000
p-ERK1/2	Cell Signaling Technology/4377	1:1000
Total Erk1/2	Santa Cruz Biotechnology/sc-93	1:5000
p-RPS6 S235	Cell Signaling Technology/2211	1:1000
Total rpS6	Cell Signaling Technology/2217	1:1000
p-eEF2 T56	kind gift of C. Proud, Univ. of Southampton, UK	1:1000
total eEF2	Cell Signaling Technology/2332	1:1000

Supplementary Methods

Animals

All mice (C57BL/6) were maintained in a temperature (25°C), humidity (50-60%), light-controlled (12hr light/dark cycle), and pathogen-free environment. Animal protocols were approved for use by the University of Massachusetts Medical School Institutional Animal Care and Use Committee (IACUC).

Biochemical analyses and Western Blotting

Co-immunoprecipitations were performed using mouse brains or Neuro2A cells transfected with pcDNA-CPEB-HA as described¹⁸. Mouse monoclonal anti-HA (Covance), and rabbit polyclonal anti-FMRP (Abcam) antibodies were used for immunoprecipitation. For Western blot analysis, the hippocampus was rapidly dissected on ice from P28-35 male mice of the indicated genotypes, rinsed briefly in 1xHBSS, then rapidly lysed in ice cold lysis buffer (in mM: 10 Hepes pH7.4, 2 EDTA, 2 EGTA, plus 1% Triton-X100, with protease (Roche) and phosphatase (CalBiochem) inhibitors). Samples were quantified by Coomassie Protein Assay (ThermoFisher), and 10 µg loaded per lane onto 6% or 12% Tris-glycine SDS-PAGE gels, transferred to PVDF and blotted with the antibodies indicated in Supplementary Table 6.

Slice labeling

Metabolic labeling experiments were performed as described¹¹, except as noted below. Briefly, 500 µm thick hippocampal slices were prepared from P28-30 male WT, *Fmr1* KO, *Cpeb* KO and DKO mice. Littermate pairing was not possible given the genotype yield of the genetic crosses used so mice were aged matched as nearly as possible for all experiments. Slices recovered in artificial cerebrospinal fluid (ACFS, in mM: 125 NaCl, 2.5 KCl, 2 CaCl₂, 1 MgCl₂, 26 NaHCO₃, 1.25 NaH₂PO₄, 10 glucose, saturated with 95% CO₂ and 5% O₂) at 32°C for 2.5 to 3.5 hours prior to labeling. Slices were incubated in 25 µM actinomycin D (Sigma Aldrich) for 30 minutes, followed by 30 minutes of labeling in 10 µCi/mL ³⁵S-methionine labeling mix (Perkin Elmer) in ACSF. After labeling, slices were snap frozen in liquid nitrogen. Slices were thawed for processing in ice-cold homogenization buffer (HB: 10 mM HEPES pH 7.4, 2 mM EDTA, 2 mM EGTA) containing protease (Roche) and phosphatase inhibitors (EMD Biosciences). Slices were then dounce homogenized in HB + 1% Triton-X-100. Proteins were precipitated with 10% trichloroacetic acid (TCA) on ice for 10 minutes. Protein pellets were resuspended in 1N NaOH, then neutralized with HCl before aliquots were taken for scintillation counting and protein concentration assays as described. Radioactivity, as expressed in counts per minute per µg of protein, were normalized to the incorporation of the WT animal for each experiment.

Long Term Depression (LTD) Analysis

Brains from mice 6-7 weeks of age with the indicated genotypes were quickly removed and placed in ice-cold cutting solution (CS) composed of (in mM): 110 sucrose, 60 NaCl, 3 KCl, 1.25 NaH₂PO₄, 28 NaHCO₃, 0.5 CaCl₂, 7 MgCl₂, 5 D-glucose, and 0.6 ascorbate. Transverse hippocampal slices (400 µm) were prepared using a Leica VT1200 Vibratome (Leica, Bannockburn, IL). The slices were allowed to recover for 30 min at room temperature in 50:50 CS:ACSF, followed by additional recovery for 30 minutes in room-temperature ACSF.

After initial recovery, the slices were placed in an interface chamber (Scientific Systems Design, Mississauga, Ontario, Canada) and maintained at 32°C in ACSF (2 mL/min). The slices were allowed to recover for an additional 120 min on the electrophysiology rig prior to experimentation. All solutions were constantly aerated with 95% O₂ + 5% CO₂. Bipolar stimulating electrodes (92:8 Pt:Y) were placed at the border of area CA3 and area CA1 along the Schaffer-Collateral pathway. ACSF-filled glass recording electrodes (1–3 MΩ) were placed in the stratum radiatum of area CA1. Basal synaptic transmission was assessed for each slice by applying gradually increasing stimuli (0.5–15V), using a stimulus isolator (A-M Systems, Carlsborg, WA) and determining the input:output relationship. All subsequent stimuli applied to slices were equivalent to the level necessary to evoke a fEPSP that was 50% of the maximal initial slope that could be evoked. Synaptic efficacy was continuously monitored (0.05 Hz) and sweeps were averaged together every 2 min. fEPSPs were amplified (A-M Systems Model 1800) and digitized (Digidata 1440, Molecular Devices, Sunnyvale, CA) prior to analysis (pClamp, Molecular Devices, Sunnyvale, CA). A stable baseline synaptic transmission was established for at least 20 min. Once a stable baseline was established, the slices were treated with DHPG (50 μM) to induce long-term depression (LTD). The initial slopes of the fEPSPs from averaged traces were normalized to those obtained during the baseline recording. In some of the experiments, anisomycin (20 μM) was applied in the perfused ACSF for 20 minutes before, during, and 30 minutes after the application of DHPG (50μM).

Long Term Potentiation (LTP) Analysis

Transverse hippocampal slices (400 μm) were obtained from adult (2.5-5 months old) mice. All procedures were performed in compliance with the Institutional Animal Care and Use Committee of the State University of New York, Downstate Medical Center. Slices were cut in ice cold artificial cerebrospinal fluid (ACSF containing: (mM) 119 NaCl, 4.0 KCl, 1.5 MgSO₄, 2.5 CaCl₂, 26.2 NaHCO₃, 1 NaH₂PO₄ and 11 Glucose saturated with 95% O₂, 5% CO₂) and then warmed in oxygenated ACSF to 35°C for 45 min. Slices were thereafter allowed to equilibrate for at least 60 min in oxygenated ACSF at room temperature. For experiments, slices were immersed in a submerged recording chamber subfused with oxygenated ACSF at 35-36°C. Field excitatory postsynaptic potentials (fEPSP) from the Dentate Gyrus (DG) area were obtained via stimulation with bipolar electrodes (FHC & Co, ME, USA) and recording with borosilicate glass pipettes (5-10 mΩ) filled with ACSF solution. Responses from Schaffer collateral to CA1 cell synapses were obtained with a pair of stimulation and recording electrodes located in CA1 *stratum radiatum*. Test pulse intensity was set at approximately 40% of the maximum fEPSP slope. Test sampling was 0.017 Hz (once per minute) and test pulse duration was 50 μsec. LTP was induced by theta burst stimulation (TBS): three bursts spaced by 20 seconds, each burst consisting of six trains of high frequency stimulus (6 pulses at 100 Hz) delivered at 10 Hz.

Spine Density Analysis

Spines on primary apical dendrites of hippocampal CA1 pyramidal neurons were analyzed using the Golgi-Cox method as described previously³¹. In this study, an apical dendrite originating directly from the cell soma was classified as the main shaft and any branch arising from the main shaft is considered as the apical dendrite. Apical dendrites originating within 50-150μm of the cell soma were chosen for spine-density analysis. By using NeuroLucida system (100x, 1.3 numerical aperture, Olympus BX61), all protrusions, irrespective of their morphological characteristics, were counted as spines if they were in direct continuity with the main shaft. Spines were counted for a length of 60μm. This total length of 60μm was further subjected to a detailed segmental analysis, which

consisted of counting the number of spines in successive steps of 10 μ m each, for a total of 6 steps. Values for the number of spines from each 10 μ m segment, at a given distance from the origin of the branch, were then averaged across all neurons in a particular experimental group.

Neuron culture and immunocytochemistry

For CPEB and FMRP co-localization experiments, primary hippocampal neurons were cultured from E18 rat embryos as described³². For immunofluorescence, cultured hippocampal neurons (DIV 14-21) were fixed in 4% PFA and processed with mouse anti-FMRP (IC3, Millipore) together with rabbit anti-CPEB (ABR reagents) or rabbit anti-ZBP1 or rabbit anti-CPSF. Neurons were imaged by widefield epifluorescence microscopy with 60X oil objective on a Nikon TE Eclipse inverted microscope equipped with a motorized stage. Optical sections were captured with Z interval of 0.15 μ m using IP lab acquisition software. Image analysis was performed using Imaris(Bitplane) 3D Coloc module. A focused stack of 5 slices were subjected to quantification of co-localization by iterative randomization of one channel and co-localizing it with another to obtain an 'auto threshold' above which true co-localization was observed. To normalize dendrites from multiple neurons in the same experiment, a 'common threshold' above the autothreshold of all dendrites was chosen for each channel; the co-localization of all dendrites at which was used get an average % co-localization for the experiment. For *in vitro* synapse formation analysis, hippocampal or cortical neurons were cultured and synapsin staining was performed as described²². Neurons were imaged on a Nikon E600 Eclipse inverted fluorescence microscope equipped with a Model 18.2 color digital camera and SPOT software (Diagnostic Instruments). Images were analyzed using ImageJ.

Ribosome Transit Rate (RTR) Assay

The brain was rapidly removed from P28-35 mice, rinsed in ice cold 1X HBSS + 10mM HEPES-KOH, rapidly dissected on ice to remove the cerebellum and midbrain (subsequently discarded), and the remaining tissue homogenized in 1 mL lysis buffer³³ (25mM HEPES-KOH pH7.4, 50mM KCl, 1.5mM MgCl₂, 0.5mM DTT, plus EDTA-free protease inhibitor tablet (Roche) and 40units/mL RNase OUT (Invitrogen/Life Technologies), in a 2mL glass dounce homogenizer, 20 strokes loose, 20 strokes tight), and centrifuged at low speed (2000xg 10 min) to pellet insoluble material. To the resulting supernatant was added a creatine-based ATP regenerating mix (in mM: 125 HEPES-KOH pH7.4, 10 ATP, 2 GTP, 100 creatine phosphate, 2 spermidine, plus 1mg/mL creatine phosphokinase), 0.2 mM amino acids (less cys/met) and ³⁵S-methionine/cysteine. For control experiments, 2 μ M hippuristanol was also added³⁴. The lysate was then warmed to 30°C and samples were taken at indicated time points for SDS-PAGE. ³⁵S-labeled amino acid incorporation was assessed by phosphorimaging of SDS-PAGE gels. The relative amount of phosphor signal at 60-100 kDa was quantified in each lane using Image J and plotted as a percentage of the maximum (40 min) time point.

Audiogenic Seizure

Mice (P19-21) were individually habituated in a behavioral chamber made of transparent plastic for 2 min and were subjected to acoustic stimulus (125db at 0.25m) using a personal alarm (Radioshack, 49-1010) for 2 min. All assays were carried out between 4pm and 6pm. Audiogenic seizure phenotypes consisting of sequential responses of wild running, seizure, and status epilepticus, or death were noted.

T-Maze

This test was used to measure working memory performance in rodents^{35,36}. The maze consisted of 3 equally sized arms (30 cm x 7.5 cm x 30 cm high) made from white plastic: one start-arm leading in a 90° angle to the two target arms (opposing each other). All arms were equipped with sliding doors. During the test, mice were first confined in the start-arm. Once the door of this arm was opened the mouse was allowed to choose one of the target arms. The door of the opposing target-arm was closed until the mouse returned to the start arm. The protocol was repeated until the mouse had made 15 choices. Additionally, the time that a mouse needed to complete this task was measured. To analyze working memory performance, the number of alternations between the target arms were counted.

Open field test

This test was used to measure locomotor activity and anxiety in mice^{23,37,38}. The apparatus consisted of an arena (40 x 40 cm) surrounded by 30 cm high walls made of white plastic. The arena was illuminated with white light (350 lux). Mice were individually placed into the arena and allowed to explore the arena for 15 min. The total distance moved, indicative of locomotor activity, and the time spent in a virtual center (15 x 15 cm) of the open field to evaluate anxiety related behavior, were determined. Behavior of the mice was tracked with the video-based EthoVision system (Noldus, Wageningen, The Netherlands).

Passive Avoidance Test

To measure long-term memory, a passive avoidance paradigm was employed³⁹⁻⁴¹. The experiments were performed in a two-chamber passive avoidance box (Gemini, San Diego Instruments, San Diego, CA). Both boxes were equipped with a steel rod floor (20.5 cm x 25 cm surface) and interconnected by a sliding door. One box was not illuminated (≤ 10 lux) and the other box was illuminated with white light (250 lux). Mice were placed in the light compartment and left there for 1 min; the door separating the two compartments was then opened and the latency to enter the dark compartment was determined. The door was then closed and the mice received a foot-shock (1s, 0.25 mA); they were returned thereafter to their home cage. The same procedure was repeated 24 h later, but in the absence of a foot-shock.

Home cage activity

Mice were individually housed for at least 3 days in a standard macrolon mouse cage (18 x 29 cm, 12 cm high) to ensure that they would perceive the cage as their home cage. They were then placed with their home cage into one frame of a photobeam activity system for home cage (San Diego Instruments, San Diego, CA). Activity was measured continuously for 24 h. For visual representation, the locomotor activity data for each hour were summarized.

Nesting Assay

Nest building was assessed essentially as described⁴² with the following changes: Animals were single-housed with a 2.5g Nestlet and left undisturbed for 72 hours. Nests were assessed and unused Nestlet weighed, then a fresh Nestlet was placed in the cage. A second assessment was performed 24 hours later.

Bilateral Hippocampal Injection

To deliver *Cpeb* siRNA into the dorsal hippocampus, P39–P44 *Fmr1* knockout mice were anesthetized with a ketamine (100 mg/kg)/xylazine (10 mg/kg) mixture administered intraperitoneally, and thereafter placed on a stereotactic frame (Stoelting) equipped with a mouse adapter. Bilateral injection coordinates according to the mouse brain atlas⁴³ were (from bregma) -1.5 mm anteroposterior (AP), ±1 mm mediolateral (ML), and 1.5 mm dorsoventral (DV). A 10 µl Hamilton syringe was used to inject 1 µL (0.25 µL/min) of PBS containing sh-*Cpeb*-GFP or control packaged lentivirus per hemisphere. shRNA plasmids and lentivirus were prepared as described¹⁸. After each injection, the syringe was left in place for 4 min to prevent backflow. Ten days after surgery, mice were tested in the T-Maze. After completion of the tests brains were dissected and the knockdown efficacy of GFP-containing tissue was determined by RT-qPCR. Based on previous hippocampal injections with lentivirus, we estimate approximately 50% of cells in the GFP-containing region of the brain were infected¹⁸.

Statistics

LTD data were analyzed by two-way RM-ANOVA analysis. LTP data were analyzed with a two-way repeated measured ANOVA test followed by a post-hoc analysis for three independent populations between series of control and knock out groups (SigmaStat 3.5; Systat Software Inc., Germany). Spine density was analyzed by one way-ANOVA. Behavioral data were analyzed with the two-way ANOVA followed by post-hoc analysis when appropriate. In cases where the data were not normally distributed as determined by Levene's test, they were analyzed with the non-parametric Mann-Whitney test. Western blot data were analyzed by student's t test (WT vs. respective genotype). In all cases, the determination of statistical significance was set to $p < 0.05$.

Bioinformatic identification of CPEB targets

To identify putative CPEB target mRNAs, mouse Refseq gene annotations of FMRP-CLIP targets⁵ were downloaded from UCSC and processed to define their 3'UTR coordinates. Of the 842 FMRP-CLIP targets, 827 were found to have annotated Refseq 3'UTRs. The corresponding genomic sequences (mm9) of these regions were then searched for the presence of CPEs UUUUAAU and UUUUUAU. An FMRP target containing one or more of these motifs within its terminal nucleotides (up to 300 nucleotides upstream of the annotated transcription end) was considered a potential CPEB target. Generally this placed the CPE within 200-250 nucleotides from the cleavage and polyadenylation signal (AAUAAA)⁴⁴.

Additional References

31. Raju, R. T. & Rao, B. S. S. *Brain and Behavior*. 108–111 (National Institute of Mental Health and Neurosciences, Bangalore, India).
32. Antar, L. N., Afroz, R., Dichtenberg, J. B., Carroll, R. C. & Bassell, G. J. Metabotropic glutamate receptor activation regulates fragile x mental retardation protein and FMR1 mRNA localization differentially in dendrites and at synapses. *J Neurosci* **24**, 2648–2655 (2004).
33. Svitkin, Y. V. & Sonenberg, N. A highly efficient and robust in vitro translation system for expression of picornavirus and hepatitis C virus RNA genomes. *Methods Enzymol* **429**, 53–82 (2007).
34. Bordeleau, M.-E. *et al.* Functional characterization of IRESes by an inhibitor of the RNA helicase eIF4A. *Nat Chem Biol* **2**, 213–220 (2006).
35. Deacon, R. M. J. & Rawlins, J. N. P. T-maze alternation in the rodent. *Nat Protoc* **1**, 7–12 (2006).
36. Brito, L. S., Yamasaki, E. N., Paumgarten, F. J. & Brito, G. N. Continuous and discrete T-maze alternation in rats: effects of intertrial and interrun intervals. *Braz J Med Biol Res* **20**, 125–135

- (1987).
37. Engin, E. & Treit, D. The role of hippocampus in anxiety: intracerebral infusion studies. *Behav Pharmacol* **18**, 365–374 (2007).
 38. Ramos, A. & Mormede, P. Stress and emotionality: a multidimensional and genetic approach. *Neurosci Biobehav Rev* **22**, 33–57 (1998).
 39. Baarendse, P. J. J. *et al.* Differential involvement of the dorsal hippocampus in passive avoidance in C57bl/6J and DBA/2J mice. *Hippocampus* **18**, 11–19 (2008).
 40. Morellini, F. & Schachner, M. Enhanced novelty-induced activity, reduced anxiety, delayed resynchronization to daylight reversal and weaker muscle strength in tenascin-C-deficient mice. *Eur J Neurosci* **23**, 1255–1268 (2006).
 41. Morellini, F. *et al.* Improved reversal learning and working memory and enhanced reactivity to novelty in mice with enhanced GABAergic innervation in the dentate gyrus. *Cereb Cortex* **20**, 2712–2727 (2010).
 42. Deacon, R. M. J. Assessing nest building in mice. *Nat Protoc* **1**, 1117–1119 (2006).
 43. Paxinos, G. & Franklin, K. B. J. *The Mouse Brain in Stereotaxic Coordinates*. (Academic Press, 2001).
 44. McGrew, L. L. & Richter, J. D. Translational control by cytoplasmic polyadenylation during *Xenopus* oocyte maturation: characterization of cis and trans elements and regulation by cyclin/MPF. *EMBO J* **9**, 3743–3751 (1990).

Supplementary Table 1: Putative CPEs within FMRP target mRNA 3' UTRs (see Excel file)